

Theoretical fabrication of Williamson nanoliquid over a stretchable surface

Humaira Sharif¹, Muzamal Hussain^{*1}, Mohamed Amine Khadimallah²,
Hamdi Aayed^{3,4}, Muhammad Taj⁵, Javed Khan Bhutto⁶, S.R. Mahmoud⁷,
Zafer Iqbal^{8,9}, Shabbir Ahmad¹⁰ and Abdelouahed Tounsi^{11,12}

¹ Department of Mathematics, Govt. College University Faisalabad, 38040, Faisalabad, Pakistan

² Prince Sattam Bin Abdulaziz University, College of Engineering, Civil Engineering Department, Al-Kharj, 16273, Saudi Arabia

³ Department of Civil Engineering, College of Engineering, King Khalid University, Abha, Saudi Arabia

⁴ Higher Institute of Transport and Logistics of Sousse, University Sousse, Tunisia

⁵ Department of Mathematics, University of Azad Jammu and Kashmir, Muzaffarabad, 1300, Azad Kashmir, Pakistan

⁶ Electrical Engineering Department, College of Engineering, King Khalid University, Abha 61421, Saudi Arabia

⁷ GRC Department, Faculty of Applied Studies, King Abdulaziz University, Jeddah, Saudi Arabia

⁸ Department of Mathematics, University of Sargodha, Sargodha, Punjab, Pakistan

⁹ Department of Mathematics, University of Mianwali, Punjab, Pakistan

¹⁰ Department of Mathematics, COMSATS University Islamabad, Lahore Campus, Pakistan

¹¹ YFL (Yonsei Frontier Lab), Yonsei University, Seoul, Korea

¹² Department of Civil and Environmental Engineering, King Fahd University of Petroleum and Minerals, 31261 Dhahran, Eastern Province, Saudi Arabia

(Received June 25, 2020, Revised June 11, 2022, Accepted August 21, 2022)

Abstract. On the basis of fabrication, the utilization of nano material in numerous industrial and technological system, obtained the utmost significance in current decade. Therefore, the current investigation presents a theoretical disposition regarding the flow of electric conducting Williamson nanoliquid over a stretchable surface in the presence of the motile microorganism. The impact of thermal radiation and magnetic parameter are incorporated in the energy equation. The concentration field is modified by adding the influence of chemical reaction. Moreover, the splendid features of nanofluid are displayed by utilizing the thermophoresis and Brownian motion aspects. Compatible similarity transformation is imposed on the equations governing the problem to derive the dimensionless ordinary differential equations. The Homotopy analysis method has been implemented to find the analytic solution of the obtained differential equations. The implications of specific parameters on profiles of velocity, temperature, concentration and motile microorganism density are investigated graphically. Moreover, coefficient of skin friction, Nusselt number, Sherwood number and density of motile number are clarified in tabular forms. It is revealed that thermal radiation, thermophoresis and Brownian motion parameters are very effective for improvement of heat transfer. The reported investigation can be used in improving the heat transfer appliances and systems of solar energy.

Keywords: Brownian motion; convective conditions; Homotopy analysis; motile micro-organism; thermal radiation; Williamson nanofluid

1. Introduction

In the past couple of decades, literature on nanofluids has expanded by taking too much attention by the researchers due to its features to enhance the thermal conductivity related to base liquids. This idea was initiated by Choi and Eastman (1995). Owing to small size and very huge for a particular surface areas of nanoparticles, Nanofluids are observed to possess increased superior properties like viscosity, thermal conductivity, thermal diffusion, and coefficients of convective transfer of heat compared with the base liquid such as ethylene glycol, water, oil, etc. Nanofluids have outstanding characteristics that make them potentially useful. Due to its use on large

scale, they have gained much attention. Usage of nanofluids are in many electronic equipment (cooling of microchips, heavy-duty engine and in industries to increase the efficiency, save energy and diminish emissions, micro-reactors, pharmaceutical procedure, transport industry) applications in bio-medical (antibacterial, delivery of nano-drug, cancer therapeutics, cryopreservation, nano-cryosurgery, realizing and imaging, etc.) and much more. Sheikholeslami *et al.* (2019b) have analyzed the problem on Variable magnetic forces influence on magnetizable hybrid nanoliquid transfer of heat through a circular cavity. Sheikholeslami *et al.* (2019a) have studied the utilization of neural system for estimation of heat transfer analysis of $Al_2O_3 - H_2O$ nanoliquid through a channel. Liang and Mudawar (2019) have presented the Review of single and two-phase nanoliquid transfer of heat in macro and micro-channels.

Pramuanjaroenkij *et al.* (2018) investigated the numerical Study of combining thermal conductivity models

*Corresponding author, Research Scholar, Ph.D.,
E-mail: muzamal45@gmail.com;
muzamalhussain@gcuf.edu.pk

for Nano liquid heat transfer increment. Kuznetsov and Nield (2010) discussed the characteristics of nanofluid in convective boundary layer flow over vertical surface. In addition to modern advancements related to the proposed observation could be determined by researchers (Rashidi *et al.* 2019, Maleki *et al.* 2019, Khan *et al.* 2019, Szilagyi *et al.* 2011, Nasiri *et al.* 2019, Nazari *et al.* 2019, Hassan *et al.* 2020). Magnetohydrodynamics is the study of magnetic field of electrically conducting fluids. Swedish physicist (Alfvén 1942), was first introduced the MHD fluid motion. MHD shows current applications in manufacturing of thermal protection, in petroleum industry, in space vehicle propulsion, in MHD pumps, in polymer technology, in heat exchanger, in electronics and chemical engineering. Many researchers (Hayat and Mehmood 2011, Nadeem *et al.* 2010, Jha and Apere 2013, Gireesha *et al.* 2015) have observed the MHD influence on flow problem including various facet. Tlili *et al.* (2022) conducted a study on transiently simulates a room with a Trombe wall on the side of the room. For this, COMSOL software has been used for simulation and numerical analysis. The wall consists of 4 rectangular blocks of PMC and 4 cement blocks with similar dimensions. The arrangement of PMC blocks and cement blocks is one in between. By moving the cement block and PCM block, two arrangements were obtained, both of which were analyzed. They observed that effect of MHD has a vital role in applications of thermal management. The convective influence of Jeffrey fluid MHD heat transfer flow over a stretchable surface is examined by Hayat *et al.* (2015). The Maxwell fluid influence of convection in MHD flow of heat transfer is analyzed by Mustafa *et al.* (2015). Alkanhal *et al.* (2019) studied the impact of thermal management of nano liquid within the permeable surface along with radiation heat source and magnetic force. In their work, they conclude enhancing the Raleigh and Radiation parameter, temperature decline gradually. Viscoelastic second-grade thin film flow in two dimensional including uniform magnetic field through a stretchable surface is investigated by Ullah *et al.* (2019). Ibáñez *et al.* (2019) inspected the optimization of magnetohydrodynamic nanofluid flow in a vertical micro channel also considering the influence of numerous parameters like thermal radiation parameter, porous media, volume fraction of nanoparticle on heat transfer and global entropy.

The impact of magnetic field on the convective transfer of heat is very significant and plays an important role in handling transfer of heat in fabricating processes where the quality of final output is dependent on the heat control. Makinde (2010) proposed a similarity solution for MHD convective flow on a vertical surface along convective boundary condition. They observed that, the temperature field enhance by enlarging Biot number. Makinde and Aziz (2010) observed that mass and transfer of heat over a vertical surface due to convective boundary conditions and magnetic field. Ayodeji *et al.* (2019) investigate the flow of MHD bio convective nanofluid through a stretchable surface with the impact of Bio-convection Peclet number and microorganism concentration. Zhang *et al.* (2022) studied the solar source, although it can reduce for energy

consumption (EC) in buildings on cold days, in the summer, its presence on the envelopes intensifies EC. In this study, two techniques were used to make better use of solar energy. In the first method, phase change material (PCM) was used on the envelopes to absorb the sun's rays, thus eliminating summer radiation problems.

For non-Newtonian fluid shear stress do not directly proportional to the deformation rate. However, liquids that do not pursue the Newton law of viscosity are known as non-Newtonian fluid. Examples of non-Newtonian fluid are shampoo, ketchup, blood, paint etc. Williamson nano liquid is also non-Newtonian fluid. Analysis of Williamson nanofluid for the flow of boundary layer has a great importance due to its large number of applications in various field of science, Engineering, technology, chemical industry, Nuclear industry, Geo physics etc. By taking these applications into consideration wide range of scientific models have been formed to promote the flow action among these non-Newtonian liquids. Flow of non-Newtonian fluid (Pseudo plastic material) and shows a model equation taken into consideration the flow of pseudo plastic liquids and justify the outcomes experimentally discussed by Williamson (1929). Mustafa *et al.* (2013) observed the effect of heat and mass transfer with flexible surface on flow of Williamson Nano liquid. Razi *et al.* (2019) observed the influence of velocity index and slip parameters with surface thickness on MHD Williamson nanofluid flow with a stretchable surface on permeable surface. Ibrahim and Gamachu (2019) examined the effect of non-linear convection Williamson nanofluid flow along stretchable surface. They indicated that temperature field and concentration field enhanced while increasing the thermophoresis parameter and magnetic field. Recently, boundary layer flow of Newtonian fluids and non-Newtonian fluids have gained much attention due to its significant utilization in preparing of metallurgical, plastic sheets, process of chemical engineering transportation etc. Transportation of heat, momentum and species plays a significant role in such procedure is observed by Kumaran and Ramanaiah (1996). Tlili *et al.* (2022) investigated the important feature of any desalination technology is energy consumption of producing fresh water specially when its energy source is solar energy. To improve this, study of various input parameters and determination of their effects on energy consumption would be essential. In this paper, a one-dimensional model is used to investigate the effects of different operational and geometrical parameters on energy consumption of flat sheet direct contact membrane distillation (DCMD) for solar desalination purposes.

Bio-convection is a captivating process of fluid mechanics that is controlled by the floating movement of living organism. A pattern of bio-convection is commonly observed by the swimming movement of small living organism which is heavier than molecule of water in suspension. When the above part of the suspension become thick due to accumulation of small living organism, it becomes imbalance and small living organism fall prey to bio-convection. Motion of nanoparticles is produced by thermophoresis parameter and Brownian motion. Motion of nano particles is free out the movement of micro-organism

so the combined interface of nano liquids and bio-convection change to be significant for micro-fluidic appliances. Makinde *et al.* (2013) observed that MHD nanofluids flow including mass and heat transfer with a vertical stretchable surface also including the effect of motile microorganisms. Khan and Pop (2010) worked on the combined effect of magnetic field and Navier slip containing micro-organism over a vertical surface including boundary layer flow of nanofluids. Numerical solution of heat and mass transfer in bio-convective flow of water base nanoliquids with motile micro-organism is observed by Siddiqua *et al.* (2016). Ayodeji *et al.* (2020) analyzed that flow of Magneto-hydrodynamics Bio-convection nano liquid Slip along a stretchable surface with Brownian motion and Thermophoresis parameter. It is noticed that increment of radiation parameter, thickness of boundary layer also increase. Several researchers used different approaches for the investigation of frequency of cylinders and concrete material (Kagimoto *et al.* 2015, Mesbah and Benzaid 2017, Alijani and Bidgoli 2018, Demir and Livaoglu 2019, Samadvand and Dehestani 2020, Qi *et al.* 2022, Alzahrani *et al.* 2022, Gao *et al.* 2022).

In this present article, our objective is to evaluate the magnetohydrodynamic flow of Williamson nanofluid in the presence of motile microorganism and chemical reaction across the horizontally stretching surface. By considering the magnetic field, motile microorganism, non-linear thermal radiation, and convective boundary conditions made this investigation very impressive and versatile. The non-dimensional boundary-value problem is tackled analytically by using the Homotopy analysis method. The impact of various pertinent parameters is discussed through tables and graphs.

2. Mathematical formulation

Considered a two-dimensional MHD boundary layer flow of an incompressible Williamson nanoliquid over a stretching surface in a permeable medium. The stretching sheet moves with uniform velocity $u = ax$, where a is positive constant. A magnetic field is imposed normal to flow. T denotes the nanofluid temperature, C is the nanofluid concentration, n the motile microorganism density. U_w represents the velocity of the fluid, T_∞ is ambient temperature, C_∞ is ambient concentration. The governing equations for Williamson nanofluid can be expressed as

$$\frac{\partial u}{\partial x} + \frac{\partial v}{\partial y} = 0 \quad (1)$$

$$\begin{aligned} & u \frac{\partial u}{\partial x} + v \frac{\partial v}{\partial y} + \alpha \left(u^2 \frac{\partial^2 u}{\partial x^2} + v^2 \frac{\partial^2 v}{\partial y^2} + 2uv \frac{\partial^2 u}{\partial x \partial y} \right) \\ & = v \frac{\partial^2 u}{\partial y^2} + \sqrt{2}v \frac{\partial u}{\partial y} \frac{\partial^2 u}{\partial y^2} - \sigma \frac{B_0^2}{\rho} u - \frac{v}{k^*} u \\ & + \frac{1}{\rho_f} [(1 - C_\infty) \rho_f \beta^{**} g(T - T_\infty) - (\rho_p - \rho_f) g(C - C_\infty) \\ & - (n - n_\infty) g\gamma^* (\rho_m - \rho_f)] \end{aligned} \quad (2)$$

$$\begin{aligned} u \frac{\partial T}{\partial x} + v \frac{\partial T}{\partial y} & = \alpha_m \left(\frac{\partial^2 T}{\partial y^2} \right) - \frac{1}{(\rho c)_p} \left(\frac{\partial q_r}{\partial y} \right) \\ & + \tau \left\{ D_B \left(\frac{\partial c}{\partial y} \frac{\partial T}{\partial y} \right) + \frac{D_T}{T_\infty} \left(\frac{\partial T}{\partial y} \right)^2 \right\} \\ & + \frac{v}{(\rho c)_p} \left(\frac{\partial u}{\partial y} \right)^2 + \frac{\sigma B_0^2}{\rho} u^2 \end{aligned} \quad (3)$$

$$u \frac{\partial C}{\partial x} + v \frac{\partial C}{\partial y} = D_B \left(\frac{\partial^2 C}{\partial y^2} \right) + \frac{D_T}{T_\infty} \left(\frac{\partial^2 T}{\partial y^2} \right) - k' \quad (4)$$

$$u \frac{\partial n}{\partial x} + v \frac{\partial n}{\partial y} + \frac{b_1 W_c}{C_w - C_\infty} \left[\frac{\partial}{\partial y} \left(n \frac{\partial C}{\partial y} \right) \right] = D_m \left(\frac{\partial^2 n}{\partial y^2} \right) \quad (5)$$

In governing expression u and v denote the nano fluid velocity components along x -axis and y -axis respectively. ρ the base fluid density, α_m represents the thermal diffusivity, D_B is Brownian diffusion coefficient, D_T is thermophoresis diffusion coefficient, $(\rho c)_p$ the heat capacitance of nano particles, $(\rho c)_f$ is heat capacitance of fluid, D_m denotes the diffusivity of microorganisms, B_0 is magnetic field, k^* stands for porous media permeability, W_c represents the maximal speed of swimming cell, τ denotes the ratio of heat capacity of nanoparticles to heat capacity of liquid.

The associated boundary conditions are

$$\begin{aligned} u & = U_w(x) = ax, & v & = 0, \\ -k \frac{\partial T}{\partial y} & = h_f(T_f - T), & D_n \frac{\partial C}{\partial y} & = k_n(C_f - C), \\ -N \frac{\partial n}{\partial y} & = l(n_f - n) \quad \text{at } y = 0, \end{aligned} \quad (6)$$

$$u \rightarrow 0, \quad T \rightarrow T_\infty, \quad C \rightarrow C_\infty, \quad n \rightarrow n_\infty \quad \text{as } y \rightarrow \infty, \quad (7)$$

Where h_f , k_n , l are respectively the coefficients of heat transfer, mass transfer microorganism density transfer.

Introducing the dimensionless similarity functions

$$\begin{aligned} \eta & = \sqrt{\frac{a}{\nu}} y, & \psi & = \sqrt{a\nu x} f(\eta), \\ g(\eta) & = \frac{T - T_\infty}{T_f - T_\infty}, & j(\eta) & = \frac{C - C_\infty}{C_f - C_\infty}, \\ \chi(\eta) & = \frac{n - n_\infty}{n_f - n_\infty}, & u & = axf'(\eta), \quad v = -\sqrt{a\nu} f(\eta), \end{aligned} \quad (8)$$

After using similarity functions Eqs. (2)-(7) transformed form as

$$f''' + ff'' - (f')^2 + W_e f'' f''' - (M + k_p) + \alpha(\theta - N_r \phi - N_c \chi) = 0 \quad (9)$$

$$\begin{aligned} \left(1 + \frac{4}{3} R_d\right) \theta'' + P_r E_c (f'')^2 + P_r f \theta' \\ + P_r N_b \theta' \phi' + P_r N_t (\theta')^2 + P_r M E_c (f')^2 = 0 \end{aligned} \quad (10)$$

$$\phi'' + L_e f \phi' + \frac{N_t}{N_b} \theta'' - L_e \beta \phi = 0 \quad (11)$$

$$\chi'' + L_b f \chi' - P_e [\phi''(\sigma + \chi) + \chi' \phi'] = 0 \quad (12)$$

The dimensionless form of boundary conditions is

$$\begin{aligned} f(0) = 0, \quad f'(0) = 1, \quad \theta'(0) = B_{i1}(\theta(0) - 1), \\ \phi'(0) = B_{i2}(\phi(0) - 1), \\ \chi'(0) = B_{i3}(\chi(0) - 1) \quad \text{at } \eta = 0, \end{aligned} \quad (13)$$

$$f' \rightarrow 0, \quad \theta \rightarrow 0, \quad \phi \rightarrow 0, \quad \chi \rightarrow 0 \quad \text{as } \eta \rightarrow \infty \quad (14)$$

Where $P_r = \frac{\nu}{\alpha_m}$ is Prandtl number, $R_d = \frac{4T_\infty^3 \sigma^*}{3k^*k}$ is radiation parameter, $k_p = \frac{\nu}{k^*a}$ the permeability parameter,

$W_e = \beta \chi \sqrt{\frac{2a^3}{\nu}}$ the Weissenberg number,

$\alpha = \frac{(1-C_\infty)\beta^{**}g(T_f-T_\infty)}{a^2x}$ is mixed convection parameter,

$N_r = \frac{(\rho_p - \rho_f)(C_f - C_\infty)}{\beta^{**}\rho_f(1-C_\infty)(T_f-T_\infty)}$ the buoyancy ratio parameter,

$N_c = \frac{\gamma^*(n_w - n_\infty)(\rho_m - \rho_f)}{\beta^{**}\rho_f(1-C_\infty)(T_f-T_\infty)}$ is bio-convection Rayleigh number, $\beta = \frac{k'u(C_\infty - C_f)}{\nu}$ is chemical reaction parameter,

$N_t = \frac{\tau D_T(T_f - T_\infty)}{\nu T_\infty}$ denotes the thermophoresis parameter,

$N_b = \frac{\tau D_B(C_f - C_\infty)}{\nu}$ the Brownian motion parameter, $M = \frac{\sigma B_0^2}{\rho a}$ is magnetic parameter, $L_e = \frac{\nu}{D_B}$ the Lewis number,

$E_c = \frac{(u_w)^2}{(\rho c)_f(T_f - T_\infty)}$ represents the Eckert number, $L_b = \frac{\nu}{D_m}$

is bio convection Lewis number, $P_e = \frac{bW_c}{D_m}$ is bio convection Peclet number, $\sigma = \frac{n_\infty}{n_f - n_\infty}$ is bio convection concentration difference parameter.

The vital physical quantities are skin friction coefficient, local nusselt number, local Sherwood number and local motile number which are expressed as

$$\begin{aligned} C_f = \frac{\tau_w}{\rho(ax)^2}, \quad Nu_x = \frac{xq_w}{k(T_f - T_\infty)}, \\ Sh_x = \frac{xq_m}{D_B(C_f - C_\infty)}, \quad Nn_x = \frac{xq_n}{D_m(n_f - n_\infty)} \end{aligned} \quad (15)$$

Where τ_w denotes the shear stress with the stretchable surface, q_w the heat flux of the surface, q_m is mass flux of the surface, q_n the motile microorganism flux, are given as

$$\begin{aligned} q_w = -k \left(\frac{\partial T}{\partial y} \right)_{y=0}, \quad q_m = -D_B \left(\frac{\partial C}{\partial y} \right)_{y=0}, \\ q_n = -D_m \left(\frac{\partial n}{\partial y} \right)_{y=0} \end{aligned} \quad (16)$$

Apply Eqs. (13)-(14) in (15)-(16), we obtain the following transformed form

$$\begin{aligned} C_f \sqrt{Re_x} = -f''(0) + \frac{\lambda}{2} f'^2(0), \quad \frac{Nu_x}{\sqrt{Re_x}} = -\theta'(0), \\ \frac{Sh_x}{\sqrt{Re_x}} = -\phi'(0), \quad \frac{Nn_x}{\sqrt{Re_x}} = -\chi'(0) \end{aligned} \quad (17)$$

Where $Re_x = \frac{xu_w(x)}{\nu}$ is local Reynolds number.

3. Methodology

Series solution for Eqs. (9)-(12) with boundary conditions (13) and (14) is sought with implementation of Homotopy Analysis Method (HAM). This approach gives a convenient way to verify the convergence of the solution. Moreover, it should be noticed that it delivers freedom to select auxiliary parameter and initial guess. In this procedure, the assisting parameters are utilized to control the convergence. Here $f_0(\eta)$, $\theta_0(\eta)$, $\phi_0(\eta)$ and $\chi_0(\eta)$ are initial guesses and L_f , L_θ , L_ϕ and L_χ are linear operators for the velocity, temperature, concentration and microorganism density fields.

$$\begin{aligned} f_0(\eta) = 1 - e^{-\eta}, \quad \theta_0(\eta) = \frac{B_{i1}}{1 + B_{i1}} e^{-\eta}, \\ \phi_0(\eta) = \frac{B_{i2}}{1 + B_{i2}} e^{-\eta}, \quad \chi_0(\eta) = \frac{B_{i3}}{1 + B_{i3}} e^{-\eta} \end{aligned} \quad (18)$$

$$\begin{aligned} L_f = \frac{d^3 f}{d\eta^3} - \frac{df}{d\eta}, \quad L_\theta = \frac{d^2 \theta}{d\eta^2} - \theta, \\ L_\phi = \frac{d^2 \phi}{d\eta^2} - \phi, \quad L_\chi = \frac{d^2 \chi}{d\eta^2} - \chi \end{aligned} \quad (19)$$

The above differential operators obey

$$\begin{aligned} L_f[C_1^* + C_2^* e^\eta + C_3^* e^{-\eta}] = 0, \\ L_\theta[C_4^* e^\eta + C_5^* e^{-\eta}] = 0, \\ L_\phi[C_6^* e^\eta + C_7^* e^{-\eta}] = 0, \\ L_\chi[C_8^* e^\eta + C_9^* e^{-\eta}] = 0, \end{aligned} \quad (20)$$

Where C_i^* ($i = 1 - 9$) illustrate the arbitrary constants.

4. Convergence of the HAM solution

The convergence is accelerated by \hbar_f , \hbar_θ , \hbar_ϕ and \hbar_χ (auxiliary parameters) for HAM series solution. No doubt the auxiliary parameters which gives us an easy way to accommodate and control the solution convergence. Fig. 1 depicts the \hbar curves and Fig. 1(a) indicate that the suitable range of \hbar_f is $-1.80 \leq \hbar_f \leq -0.10$, Fig. 1(b) illustrates that the suitable range of \hbar_θ is $-2.0 \leq \hbar_\theta \leq -0.10$, Fig. 1(c) represents that the suitable range of \hbar_ϕ is $-1.90 \leq \hbar_\phi \leq -0.15$, Fig. 1(d) shows that the suitable rang of \hbar_χ is $-2.0 \leq \hbar_\chi \leq -0.20$. Table 1 demonstrates the series convergence. From the Table 1 we can see that homotopy analysis method is a rapidly convergent approach.

5. Analytical results and discussion

The purpose of this part is to elaborate the impacts of various parameters of interest on the profiles of velocity, temperature, concentration and microorganism density

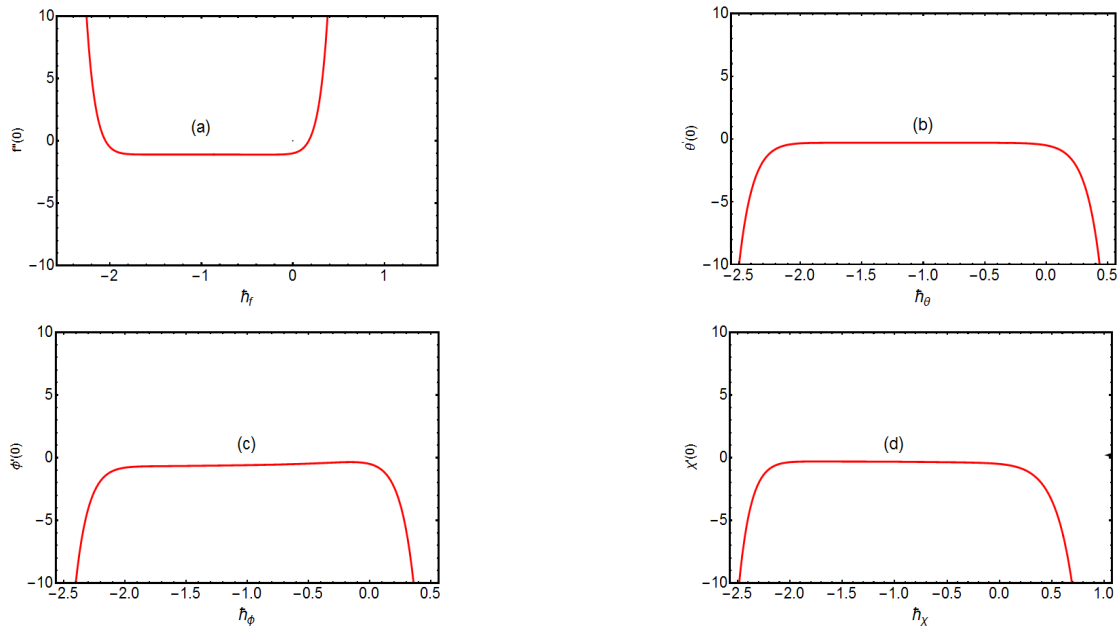


Fig. 1 Convergent h - (a) curves for velocity field; (b) temperature field; (c) concentration field; and (d) motile microorganism density field

Table 1 Convergence of Homotopy solution up to 25th order approximation where, $E_c = W_e = \sigma = \alpha = N_c = 1/10$, $N_t = N_b = N_r = 3/10$, $L_e = B_{i1} = K_p = P_r = 1$, $B_{i2} = B_{i3} = 5/10$, $L_b = 7/10$, $M = 2/10$, $\beta = Rd = 0.01$, $P_e = 9/10$

Order of approximation	$-f''(0)$	$-\theta'(0)$	$-\phi'(0)$	$-\chi'(0)$
1	1.49988	0.39933	0.28193	0.30815
6	1.53276	0.26812	0.28344	0.26175
12	1.53179	0.25525	0.32021	0.23794
16	1.53221	0.25506	0.32984	0.22808
20	1.53221	0.25490	0.33553	0.22257
23	1.53221	0.25490	0.33553	0.22257
26	1.53221	0.25490	0.33553	0.22257

through the Homotopy analysis method and these are displayed via Figs. 2-18. Fig. 2 demonstrates the influence of magnetic field parameter on dimensionless velocity profile. It is noticed that increasing the value of magnetic field parameter M fluid velocity is receded. The reason is that electrically conducting nano liquid develop a resistive force which is opposite to the fluid flow, as a result, the flow is slowed down in in the boundary layer region. Fig. 3 exhibits the impact of permeability parameter k_p on non-dimensional velocity profile, here the rising the values of permeability parameter increase Darcy resistive force which tends to slow down the flow. Fig. 4 depicts the impacts of buoyancy number N_r on velocity distribution. It is seen that the rising values of N_r , velocity curve is declined. Physically, larger values of N_r are conclusively concerned to greater bouncy force which diminishes the horizontal velocity of nanofluid. Fig. 5 portrays the influence of bio-

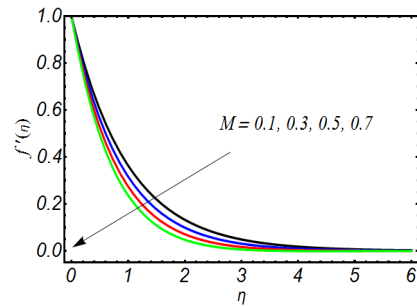


Fig. 2 Plot for influence of M on f'

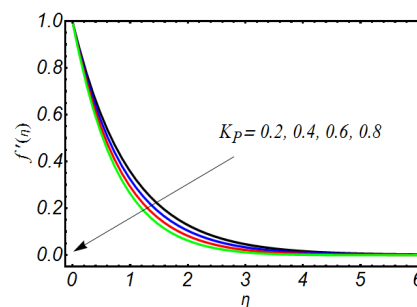


Fig. 3 Plot for influence of K_p on f'

convection Rayleigh number N_c on velocity distribution. It is observed, with the enhancing values of N_c , the velocity profile is declined. Impact of Weissenberg number W_e on flow velocity is shown in Fig. 6. It is observed that with the gradual enhancement in the values of W_e , the velocity f' goes on receding. The increasing variation of W_e represents more relaxation time and it retards the fluid motion.

Fig. 7 portrays the effect of Biot number B_{i1} on

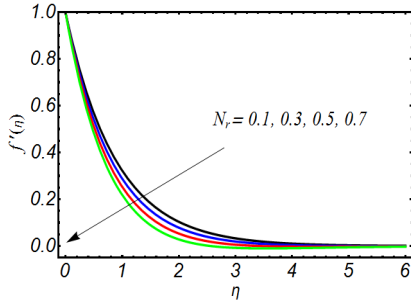


Fig. 4 Plot for influence of N_r on f'

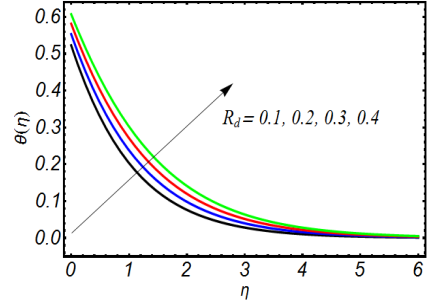


Fig. 8 Plot for influence of R_d on θ

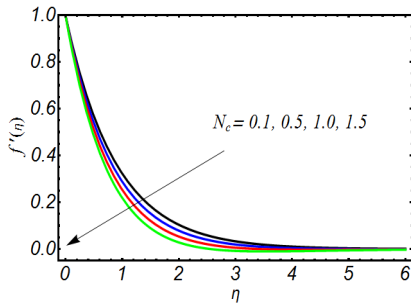


Fig. 5 Plot for influence of N_c on f'

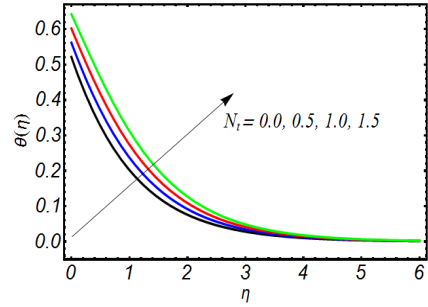


Fig. 9 Plot for influence of N_t on θ

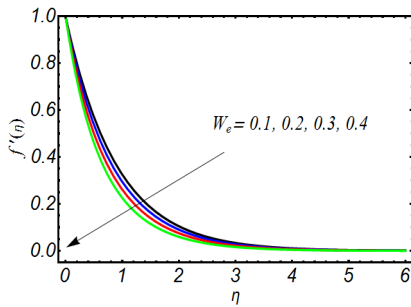


Fig. 6 Plot for influence of W_e on f'

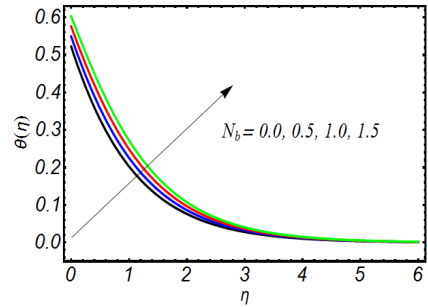


Fig. 10 Plot for influence of N_b on θ

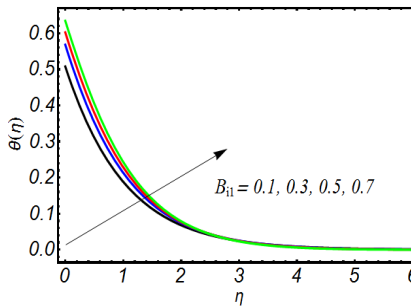


Fig. 7 Plot for influence of B_{i1} on θ

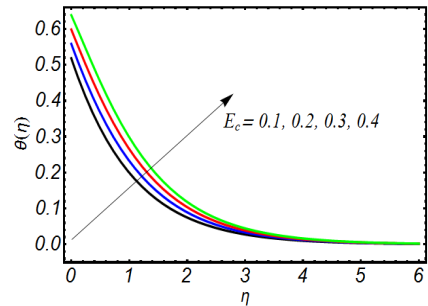


Fig. 11 Plot for influence of E_c on θ

temperature field. It is noticed that temperature of the fluid and the thickness of associative boundary layer increase with large values of Biot number. Fig. 8 shows the impact of radiation parameter R_d on the temperature field. It seems that temperature is increased directly with rising values of R_d . Thus, radiation parameter causes increment in temperature field. Actually, the increment in radiation

number leads to increasing in the kinetic energy in liquid particles, and kinetics energy causes increment in temperature of the fluid. The influence of thermophoresis parameter N_t on temperature profile is indicated in Fig. 9. It is noticed that temperature field and associated thickness of thermal boundary layer enhance with the enlarged values of N_t . According to its physical nature, the rising thermo-

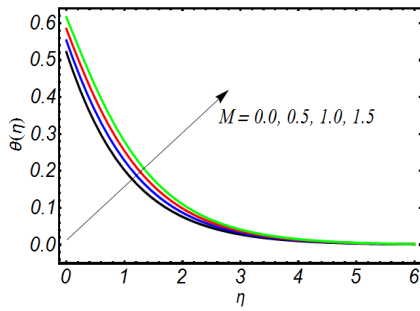


Fig. 12 Plot for influence of M on θ

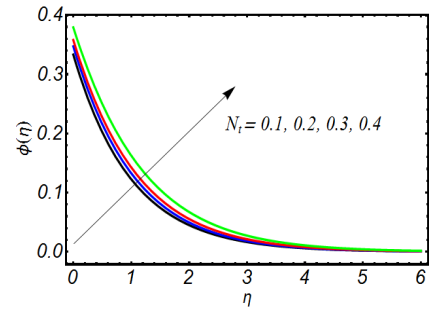


Fig. 15 Plot for influence of N_t on ϕ

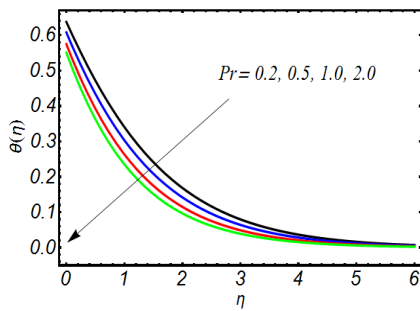


Fig. 13 Plot for influence of P_r on θ

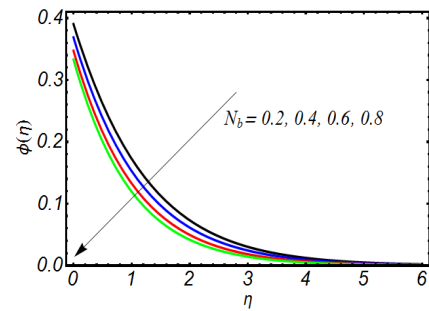


Fig. 16 Plot for influence of N_b on ϕ

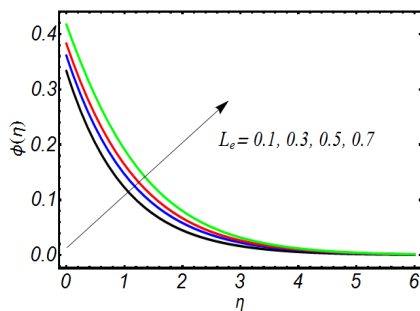


Fig. 14 Plot for influence of L_e on ϕ

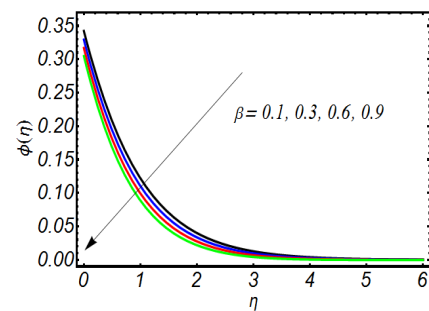


Fig. 17 Plot for influence of β on ϕ

phoresis parameter N_t means greater difference between surface temperature and reference temperature which enhances the movement of nano particles to raise the temperature field and thickness of thermal boundary layer. The behavior of Brownian motion parameter N_b on non-dimensional temperature is illustrated in Fig. 10. We noticed that the enlarged values of N_b increased the temperature field and thickness of thermal boundary. Physically, the higher values of N_b are responsible to escalate the random movement of nano particles which resulted in notable increase of the fluid temperature and thickness of boundary layer. Fig. 11 reveals that by enhancing the distinct values of Eckert number E_c raises the temperature field and thickness of boundary layer. Physically, the enlarged values of E_c correspond to more dissipation and hence it increases the generation of heat in fluid body.

Influence of magnetic parameter M is expressed in Fig. 12. It is found that for gradually increasing the values of M temperature field shows increasing behavior. This is

physically justified because electrically conducting liquid produces a Lorentz force, which is opposite to the flow, and as a result, the movement of the fluid is declined in the boundary layer and therefore temperature profile is enhanced with the increment in M . The impact of Prandtl number P_r on temperature field is shown in Fig. 13. It is noticed that temperature field has inverse relation with P_r that is temperature field declines with increasing values of P_r . The increasing values of P_r indicate the decrease in thermal conductivity therefore temperature curve is declined. Fig. 14 reflects the influence of Lewis number L_e on the concentration field. Lewis number is the ratio of thermal diffusion to the mass diffusion. It demonstrates the relationship between transfer of heat and mass coefficient. The concentration field is strengthened by enhancing the values of L_e . Fig. 15 shows the influence of thermophoresis parameter N_t on dimensionless concentration field. It is observed that large values of N_t increase the concentration field. The influence of Brownian motion parameter N_b on concentration field is analyzed in Fig. 16. The concentration

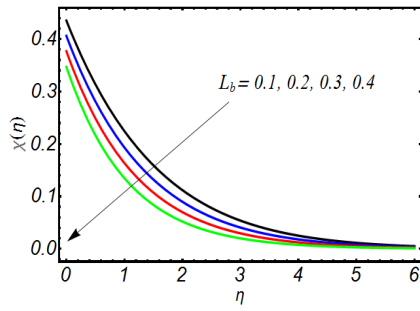


Fig. 18 Plot for influence of L_b on χ

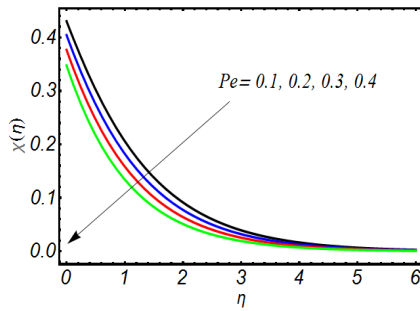


Fig. 19 Plot for influence of P_e on χ

field is declined when Brownian motion parameter increases slightly. The influence of chemical reaction coefficient β on concentration field is investigated in Fig. 17. It is observed that concentration field is diminished against the higher values of chemical reaction coefficient β . Figs. 18-19 shows the influence of bio-convective Lewis number L_b and Peclet number P_e on motile micro-organism density. It is visualized that increment in bio-

Table 2 Numerical values of the Skin friction co-efficient for various parameters where, $Le = B_{i1} = K_p = 1$, $B_{i2} = B_{i3} = 5/10$, $We = 2/10$, $N_b = N_c = E_c = \sigma = 1/10$, $\beta = Rd = 0.01$

M	N_r	α	P_r	N_t	$-C_f Re_x^{1/2}$
0.1	0.1	0.1	1.0	0.2	1.7148
0.2					1.7668
0.3					1.8181
	0.2				1.7188
	0.4				1.7270
	0.6				1.7349
		0.2			1.6728
		0.5			1.5441
		0.8			1.4263
			2.0		1.7294
			3.0		1.7361
			4.0		1.7378
				0.3	1.7220
				0.5	1.7271
				0.7	1.7319

Table 3 Nusselt number for distinct parameters where, $Le = B_{i1} = K_p = 1$, $B_{i2} = B_{i3} = 5/10$, $N_c = \sigma = 1/10$, $P_e = 3/10$, $L_b = 7/10$

R_d	P_r	N_t	N_b	E_c	β	We	$-\theta'(0)$
0.1	1.0	0.2	0.1	0.1	0.01	0.2	0.2501
							0.2091
							0.1782
	2.0						0.3193
	3.0						0.3532
	4.0						0.3741
		0.1					0.2542
		0.3					0.2413
		0.5					0.2310
			0.2				0.2483
			0.5				0.2442
			1.0				0.2294
				0.2			0.2115
				0.3			0.1693
				0.4			0.1324
					0.0		0.2109
					0.1		0.2105
					0.2		0.2102
						0.0	0.2221
						0.05	0.2185
						0.1	0.2162

Table 4 Sherwood number for different parameters where, $B_{i1} = K_p = 1$, $B_{i3} = 5/10$, $N_c = \sigma = 1/10$, $Rd = 0.01$, $P_e = 3/10$, $L_b = 7/10$

M	We	E_c	L_e	B_{i2}	N_b	$-\phi'(0)$
0.2	0.2	0.1	1.0	0.5	0.1	0.1673
0.4						0.2247
0.6						0.2416
	0.0					0.1913
	0.1					0.1985
	0.2					0.2081
		0.2				0.3747
		0.3				0.5401
		0.4				0.6772
			2.0			0.3134
			3.0			0.3840
			4.0			0.4071
				0.3		0.1161
				0.5		0.1653
				1.0		0.3071
					0.3	0.3424
					0.5	0.3706
					0.7	0.3927

Table 5 Motile micro-organism density number for various parameters. $B_{i1} = K_p = 1, B_{i2} = B_{i3} = 5/10, N_b = N_t = N_c = \sigma = 1/10, \beta = Rd = 0.01, P_e = 3/10, L_b = 7/10$

σ	L_b	P_e	$-\chi'(0)$
0.1	0.7	0.9	0.1542
0.2			0.1628
0.3			0.1721
	0.1		0.1551
	0.2		0.1725
	0.3		0.1850
		0.1	0.1594
		0.2	0.1828
		0.3	0.1909

convective Lewis number L_b and Peclet number P_e , decreases the motile microorganism density profile. The impacts of M, Nr, α, Pr and N_t on skin friction $-C_f Re_x^{1/2}$ are expressed in Table 2. It is seen that higher values of M, Nr, Pr, N_t increase $-C_f Re_x^{1/2}$ while the high values of α decreases $-C_f Re_x^{1/2}$. The variation of Nusselt number $-\theta'(0)$ for different parameters $Rd, Pr, Nb, Nt, Ec, \beta$ and We is displayed in Table 3. The behavior of Sherwood number $-\phi'(0)$ corresponding to the variation of the parameters $M, We, Ec, Le, Bi2$ and N_b is enumerated in Table 4. The response of local micro-organism density number $-\chi'(0)$ for varying values of the parameters σ, L_b and P_e is depicted in Table 5. It is noticed that enhanced values of σ, L_b and P_e has increased the local motile micro-organisms density number.

6. Conclusions

In this article, the effects of bio-convection on flow of Williamson nanofluid over a stretching surface is examined in the presence of thermal radiation, chemical reaction and convective boundary conditions. With the help of suitable substitution, different thermo-physical parameters are yielded in their non-dimensional form. The analytic solution has been found by using Homotopy analysis approach. Main results of this paper are given as below:

- By increasing the values of Weissenberg number We , permeability parameter K_p and magnetic parameter M , the flow in horizontal direction is retarded.
- The increasing the values of thermal radiation parameter Rd and Biot number B_{i1} cause rise in fluid temperature but the enhanced Prandtl number Pr , resulted in decrease of the temperature field.
- The larger Brownian motion parameter N_b , increased the temperature profile but it decreased the concentration profile.
- The temperature and concentration fields are

strengthened by increasing the values of thermophoresis parameter N_t .

- By increasing the values of bio-convection Peclet number P_e and bio-convection Lewis number L_b , the density of motile micro-organism is receded.

Declaration of conflicting interests

The author(s) declared no potential conflicts of interest with respect to the research, authorship, and/or publication of this article.

Acknowledgments

The authors extend their appreciation to the Deanship of Scientific Research at King Khalid University (KKU) for funding this work through the Research Group Program Under the Grant Number: (R.G.P.2/91/43).

ORCID ID

Muzamal Hussain

<http://orcid.org/0000-0002-6226-359X>

References

- Alfvén, H. (1942), "Existence of electromagnetic-hydrodynamic waves", *Nature*, **150**(3805), 405-406. <https://doi.org/10.1038/150405d0>
- Alijani, M. and Bidgoli, M.R. (2018), "Agglomerated SiO₂ nanoparticles reinforced-concrete foundations based on higher order shear deformation theory: Vibration analysis", *Adv. Concrete Constr., Int. J.*, **6**(6), 585-610. <https://doi.org/10.12989/acc.2018.6.6.585>
- Alkanhal, T.A., Sheikholeslami, M., Usman, M., Haq, R.U., Shafee, A., Al-Ahmadi, A.S. and Tlili, I. (2019), "Thermal management of MHD nanofluid within the porous medium enclosed in a wavy shaped cavity with square obstacle in the presence of radiation heat source", *Int. J. Heat Mass Transfer*, **139**, 87-94. <https://doi.org/10.1016/j.ijheatmasstransfer.2019.05.006>
- Alzahrani, J., Vaidya, H., Prasad, K.V., Rajashekhar, C., Mahendra, D.L. and Tlili, I. (2022), "Micro-polar fluid flow over a unique form of vertical stretching sheet: Special emphasis to temperature-dependent properties", *Case Stud. Thermal Eng.*, **34**, 102037. <https://doi.org/10.1016/j.csite.2022.102037>
- Ayodeji, F., Tope, A. and Samuel, O. (2019), "Magneto-Hydrodynamics (MHD) Bioconvection Nanofluid Slip Flow over a Stretching Sheet with Microorganism Concentration and Bioconvection Peclet Number Effects", *Am. J. Mech. Indust. Eng.*, **4**(6), 86-95. <https://doi.org/10.11648/j.ajmie.20190406.11>
- Ayodeji, F., Tope, A. and Pele, O. (2020), "Magneto-hydrodynamics (MHD) Bioconvection nanofluid slip flow over a stretching sheet with thermophoresis, viscous dissipation and brownian motion", *Mach. Learn. Res.*, **4**(4), 51. <https://doi.org/10.11648/j.mlrr.20190404.12>
- Choi, S.U. and Eastman, J.A. (1995), Enhancing thermal conductivity of fluids with nanoparticles (No. ANL/MSD/CP-84938; CONF-951135-29), Argonne National Lab., IL, USA.
- Demir, A.D. and Livaoglu, R. (2019), "The role of slenderness on

- the seismic behavior of ground-supported cylindrical silos”, *Adv. Concrete Constr., Int. J.*, **7**(2), 65-74.
<https://doi.org/10.12989/acc.2019.7.2.065>
- Gao, J., Liu, J., Yue, H., Zhao, Y., Tlili, I. and Karimipour, A. (2022), “Effects of various temperature and pressure initial conditions to predict the thermal conductivity and phase alteration duration of water based carbon hybrid nanofluids via MD approach”, *J. Molecul. Liquids*, **351**, 118654.
- Gireesha, B.J., Mahanthesh, B. and Rashidi, M.M. (2015), “MHD boundary layer heat and mass transfer of a chemically reacting Casson fluid over a permeable stretching surface with non-uniform heat source/ sink”, *Int. J. Indust. Mathe.*, **7**(3), 247-260.
- Hassan, A., Wahab, A., Qasim, M.A., Janjua, M.M., Ali, M.A., Ali, H.M., Jadoon, T.R., Ali, E., Raza, A. and Javaid, N. (2020), “Thermal management and uniform temperature regulation of photovoltaic modules using hybrid phase change materials-nanofluids system”, *Renew. Energy*, **145**, 282-293.
<https://doi.org/10.1016/j.renene.2019.05.130>
- Hayat, T. and Mehmood, O.U. (2011), “Slip effects on MHD flow of third order fluid in a planar channel”, *Commun. Nonlinear Sci. Numer. Simul.*, **16**(3), 1363-1377.
<https://doi.org/10.1016/j.cnsns.2010.06.034>
- Hayat, T., Asad, S., Mustafa, M. and Alsaedi, A. (2015), “MHD stagnation-point flow of Jeffrey fluid over a convectively heated stretching sheet”, *Comput. Fluids*, **108**, 179-185.
<https://doi.org/10.1016/j.compfluid.2014.11.016>
- Ibáñez, G., López, A., López, I., Pantoja, J., Moreira, J. and Lastres, O. (2019), “Optimization of MHD nanofluid flow in a vertical microchannel with a porous medium, nonlinear radiation heat flux, slip flow and convective-radiative boundary conditions”, *J. Thermal Anal. Calorim.*, **135**(6), 3401-3420.
<https://doi.org/10.1007/s10973-018-7558-3>
- Ibrahim, W. and Gamachu, D. (2019), “Nonlinear convection flow of Williamson nanofluid past a radially stretching surface”, *AIP Adv.*, **9**(8), 085026. <https://doi.org/10.1063/1.5113688>
- Jha, B.K. and Apere, C.A. (2013), “Unsteady MHD two-phase Couette flow of fluid-particle suspension”, *Appl. Mathe. Modell.*, **37**(4), 1920-1931.
<https://doi.org/10.1016/j.apm.2012.04.056>
- Kagimoto, H., Yasuda, Y. and Kawamura, M. (2015), “Mechanisms of ASR surface cracking in a massive concrete cylinder”, *Adv. Concrete Constr., Int. J.*, **3**(1), 39-54.
<https://doi.org/10.12989/acc.2015.3.1.039>
- Khan, W.A. and Pop, I. (2010), “Boundary-layer flow of a nanofluid past a stretching sheet”, *Int. J. Heat Mass Transfer*, **53**(11-12), 2477-2483.
<https://doi.org/10.1016/j.ijheatmasstransfer.2010.01.032>
- Khan, A., Ali, H.M., Nazir, R., Ali, R., Munir, A., Ahmad, B. and Ahmad, Z. (2019), “Experimental investigation of enhanced heat transfer of a car radiator using ZnO nanoparticles in H₂O-ethylene glycol mixture”, *J. Thermal Anal. Calorim.*, **138**(5), 3007-3021. <https://doi.org/10.1007/s10973-019-08320-7>
- Kumaran, V. and Ramanaiah, G. (1996), “A note on the flow over a stretching sheet”, *Acta Mecca*, **116**(1), 229-233.
<https://doi.org/10.35940/ijrte.c4861.098319>
- Kuznetsov, A.V. and Nield, D.A. (2010), “Natural convective boundary-layer flow of a nanofluid past a vertical plate”, *Int. J. Thermal Sci.*, **49**(2), 243-247.
<https://doi.org/10.1016/j.ijthermalsci.2009.07.015>
- Liang, G. and Mudawar, I. (2019), “Review of single-phase and two-phase nanofluid heat transfer in macro-channels and micro-channels”, *Int. J. Heat Mass Transfer*, **136**, 324-354.
<https://doi.org/10.1016/j.ijheatmasstransfer.2019.02.086>
- Makinde, O.D. (2010), “Similarity solution of hydromagnetic heat and mass transfer over a vertical plate with a convective surface boundary condition”, *Int. J. Phys. Sci.*, **5**(6), 700-710.
<http://www.academicjournals.org/IJPS>
- Makinde, O.D. and Aziz, A. (2010), “MHD mixed convection from a vertical plate embedded in a porous medium with a convective boundary condition”, *Int. J. Thermal Sci.*, **49**(9), 1813-1820. <https://doi.org/10.1016/j.ijthermalsci.2010.05.015>
- Makinde, O.D., Khan, W.A. and Khan, Z.H. (2013), “Buoyancy effects on MHD stagnation point flow and heat transfer of a nanofluid past a convectively heated stretching/shrinking sheet”, *Int. J. Heat Mass Transfer*, **62**, 526-533.
<https://doi.org/10.1016/j.ijheatmasstransfer.2013.03.049>
- Maleki, H., Safaei, M.R., Togun, H. and Dahari, M. (2019), “Heat transfer and fluid flow of pseudo-plastic nanofluid over a moving permeable plate with viscous dissipation and heat absorption/generation”, *J. Thermal Anal. Calorim.*, **135**(3), 1643-1654. <https://doi.org/10.1007/s10973-018-7559-2>
- Mesbah, H.A. and Benzaid, R. (2017), “Damage-based stress-strain model of RC cylinders wrapped with CFRP composites”, *Adv. Concrete Constr., Int. J.*, **5**(5), 539-561.
<https://doi.org/10.12989/acc.2017.5.5.539>
- Mustafa, M., Hina, S., Hayat, T. and Alsaedi, A. (2013), “Slip effects on the peristaltic motion of nanofluid in a channel with wall properties”, *J. Heat Transfer*, **135**(4).
<https://doi.org/10.1115/1.4023038>
- Mustafa, M., Khan, J.A., Hayat, T. and Alsaedi, A. (2015), “Sakiadis flow of Maxwell fluid considering magnetic field and convective boundary conditions”, *Aip Adv.*, **5**(2), 027106.
<https://doi.org/10.1063/1.4907927>
- Nadeem, S., Hussain, M. and Naz, M. (2010), “MHD stagnation flow of a micropolar fluid through a porous medium”, *Meccanica*, **45**(6), 869-880.
<https://doi.org/10.1007/s11012-010-9297-9>
- Nasiri, H., Jamalabadi, M.Y.A., Sadeghi, R., Safaei, M.R., Nguyen, T.K. and Shadloo, M.S. (2019), “A smoothed particle hydrodynamics approach for numerical simulation of nano-fluid flows”, *J. Thermal Anal. Calorim.*, **135**(3), 1733-1741.
<https://doi.org/10.1007/s10973-018-7022-4>
- Nazari, S., Ellahi, R., Sarafraz, M.M., Safaei, M., Asgari, A. and Akbari, O.A. (2019), “Numerical study on mixed convection of a non-Newtonian nanofluid with porous media in a two lid-driven square cavity”, *J. Thermal Anal. Calorim.*, 1-25.
<https://doi.org/10.1007/s10973-019-08841-1>
- Pramuanjaroenkij, A., Tongkratoke, A. and Kakaç, S. (2018), “Numerical study of mixing thermal conductivity models for nanofluid heat transfer enhancement”, *J. Eng. Phys. Thermophys.*, **91**(1), 104-114.
<https://doi.org/10.1007/s10891-018-1724-0>
- Qi, X., Sidi, M.O., Tlili, I., Ibrahim, T.K., Elkotb, M.A., El-Shorbagy, M.A. and Li, Z. (2022), “Optimization and sensitivity analysis of extended surfaces during melting and freezing of phase changing materials in cylindrical Lithium-ion battery cooling”, *J. Energy Storage*, **51**, 104545.
<https://doi.org/10.1016/j.est.2022.104545>
- Rashidi, S., Javadi, P. and Esfahani, J.A. (2019), “Second law of thermodynamics analysis for nanofluid turbulent flow inside a solar heater with the ribbed absorber plate”, *J. Thermal Anal. Calorim.*, **135**(1), 551-563.
<https://doi.org/10.1007/s10973-018-7164-4>
- Razi, S.M., Soid, S.K., Aziz, A.S.A., Adli, N. and Ali, Z.M. (2019), “Williamson nanofluid flow over a stretching sheet with varied wall thickness and slip effects”, In: *Journal of Physics: Conference Series*, Vol. 1366, No. 1, p. 012007.
<https://doi.org/10.1088/1742-6596/1366/1/012007>
- Samadvand, H. and Dehestani, M. (2020), “A stress-function variational approach toward CFRP-concrete interfacial stresses in bonded joints”, *Adv. Concrete Constr., Int. J.*, **9**(1), 43-54.
<https://doi.org/10.12989/acc.2020.9.1.043>
- Sheikholeslami, M., Gerdroodbary, M.B., Moradi, R., Shafee, A. and Li, Z. (2019a), “Application of Neural Network for

- estimation of heat transfer treatment of $\text{Al}_2\text{O}_3\text{-H}_2\text{O}$ nanofluid through a channel”, *Comput. Methods Appl. Mech. Eng.*, **344**, 1-12. <https://doi.org/10.1016/j.cma.2018.09.025>
- Sheikholeslami, M., Mehryan, S.A.M., Shafee, A. and Sheremet, M.A. (2019b), “Variable magnetic forces impact on magnetizable hybrid nanofluid heat transfer through a circular cavity”, *J. Molecular Liquids*, **277**, 388-396. <https://doi.org/10.1016/j.molliq.2018.12.104>
- Siddiq, S., Begum, N., Saleem, S., Hossain, M.A. and Gorla, R.S.R. (2016), “Numerical solutions of nanofluid bioconvection due to gyrotactic microorganisms along a vertical wavy cone”, *Int. J. Heat Mass Transfer*, **101**, 608-613. <https://doi.org/10.1016/j.ijheatmasstransfer.2016.05.076>
- Szilágyi, I.M., Santala, E., Heikkilä, M., Kemell, M., Nikitin, T., Khriachtchev, L., Räsänen, M., Ritala, M. and Leskelä, M. (2011), “Thermal study on electrospun polyvinylpyrrolidone/ammonium metatungstate nanofibers: optimising the annealing conditions for obtaining WO_3 nanofibers”, *J. Thermal Anal. Calorim.*, **105**(1), 73. <https://doi.org/10.1007/s10973-011-1631-5>
- Tlili, I. and Alharbi, T. (2022), “Investigation into the effect of changing the size of the air quality and stream to the trombe wall for two different arrangements of rectangular blocks of phase change material in this wall”, *J. Build. Eng.*, **52**, 104328. <https://doi.org/10.1016/j.job.2022.104328>
- Tlili, I., Sajadi, S.M., Baleanu, D. and Ghaemi, F. (2022), “Flat sheet direct contact membrane distillation study to decrease the energy demand for solar desalination purposes”, *Sustain. Energy Technol. Assessm.*, **52**, 102100. <https://doi.org/10.1016/j.seta.2022.102100>
- Ullah, A., Shah, Z., Kumam, P., Ayaz, M., Islam, S. and Jameel, M. (2019), “Viscoelastic MHD nanofluid thin film flow over an unsteady vertical stretching sheet with entropy generation”, *Processes*, **7**(5), 262. <https://doi.org/10.3390/pr7050262>
- Williamson, R.V. (1929), “The flow of pseudoplastic materials”, *Indust. Eng. Chem.*, **21**(11), 1108-1111. <https://doi.org/10.1021/ie5023>
- Zhang, J., Sajadi, S.M., Chen, Y., Tlili, I. and Fagiry, M.A. (2022), “Effects of Al_2O_3 and TiO_2 nanoparticles in order to reduce the energy demand in the conventional buildings by integrating the solar collectors and phase change materials”, *Sustain. Energy Technol. Assessm.*, **52**, 102114. <https://doi.org/10.1016/j.seta.2022.102114>